



## Tribological, Thermal and Kinetic Attributes of 300 vs. 450 mm Chemical Mechanical Planarization Processes

Yubo Jiao,<sup>a,z</sup> Xiaoyan Liao,<sup>a</sup> Changhong Wu,<sup>a</sup> Siannie Theng,<sup>b</sup> Yun Zhuang,<sup>a,b</sup>  
Yasa Sampurno,<sup>a,b</sup> Michael Goldstein,<sup>c,\*</sup> and Ara Philipossian<sup>a,b</sup>

<sup>a</sup>Department of Chemical and Environmental Engineering, University of Arizona, Tucson, Arizona 85721, USA

<sup>b</sup>Araca, Inc., Tucson, Arizona 85718, USA

<sup>c</sup>Intel Corporation, Santa Clara, California 95052, USA

An existing 300 mm CMP tool has been modified to polish 450 mm wafers in order to demonstrate experimentally whether any differences exist in the tribological and thermal characteristics of the two processes, and from that, to infer whether one can expect any removal rate differences between the two systems. Results suggest that, within the ranges of parameter investigated, the two systems behave similarly in terms of their coefficients of friction and lubrication regimes. Additionally, it is shown that the 450 mm process, once adjusted for its platen velocity, runs only slightly warmer (by 1–3°C) than its 300 mm counterpart. Experimental data, coupled with copper removal rate simulations show that the wafer surface reaction temperature of the 450 mm process is slightly higher (by 1–2°C) than the 300 mm process. Consequently, simulated copper removal rates for the 450 mm process are slightly higher (2–13%) than those of the 300 mm process at most polishing conditions. The above results indicate that when the current 300 mm CMP process is scaled up to 450 mm, the tribological, thermal, and kinetic attributes of the process remain similar and do not undergo significant changes.

© 2012 The Electrochemical Society. [DOI: 10.1149/2.044203jes] All rights reserved.

Manuscript submitted October 13, 2011; revised manuscript received December 1, 2011. Published January 3, 2012.

Several integrated circuit (IC) makers have announced plans for adopting 450 mm wafers which would involve a significant investment in tools and fabrication facilities.<sup>1–3</sup> M. Watanabe and J. S. Pettinato have discussed certain scaling issues associated with adopting 450 mm silicon wafers, and technology decisions to minimize the transition risks associated with 450 mm wafers, respectively.<sup>4,5</sup> Our research team has previously investigated several key questions resulting from such a possible scale-up by simulating hypothetical 300 and 450 mm processes on rotary polishers.<sup>6</sup> Using our proprietary 3D thermal model, we have been able to simulate frictional heat generation by the wafer and retaining ring and the transport and transfer of heat throughout the tool by the slurry and by the rotation of the polishing head and the platen. The simulation results<sup>6</sup> have shown that wafer temperature distribution for 450 mm is a smooth extension of the distribution for 300 mm wafers. That is, wafer body temperature does not change appreciably with scale-up. On the other hand, temperature rise in contacting pad summits, or the surface reaction temperature increment,<sup>7</sup> has been shown to be different between the two systems. Most of the heat in CMP is generated at the contact points between pad summits and the wafer or the retaining ring. Mechanically mediated material removal of chemical reaction products formed on the wafer also occurs at the contacts. Since the real contact area is often less than 0.1% of the wafer area,<sup>8</sup> contacting pad summits are probably hotter than the wafer and their temperature may therefore dominate the chemistry. Since summits spend more time in contact with the ring and wafer on a 450 mm tool due to the lower platen rotation rate (lowering the rotation rate is necessary since the 450 mm process has a larger platen diameter, therefore a slower platen rotation achieves comparable linear velocity as the 300 mm system), the wafer surface reaction temperature increment for 450 mm is expected to be higher than the 300 mm tool which theoretically should increase removal rate depending on the activation energy of the process.

In this study, we have mechanically modified an existing 300 mm polisher to polish both 300 and 450 mm bare silicon wafers, and demonstrate experimentally whether any differences exist in the tribological and thermal characteristics of the two processes. Even though no removal rate tests are performed, inferences are made regarding removal rate differences between the two systems by coupling their

tribological and thermal fingerprints with highly successful kinetics models<sup>7,9–11</sup> for copper removal.

### Experimental

All tests are performed on an Araca APD-800 polisher and tribometer which is uniquely suitable for acquiring real-time shear force and down force during polishing.<sup>12</sup> In order to accommodate both 300 and 450 mm wafers, an interface module (480 mm in diameter) made of anodized aluminum is manufactured and attached to the carrier (Fig. 1). The back side of the interface module is fitted with an o-ring which ensures a secure fit onto the carrier head using the existing vacuum conditions in the head. In addition, 300 or 450 mm compatible backing films and retaining ring assemblies are attached onto the front side of the interface module. The wetted backing film is used to securely hold the proper size wafer via capillary forces (Fig. 1). It is important to note that the APD-800's platen is 800 mm in diameter. In this study, we have opted to use a pad having a diameter of 762 mm. Since no adjustments are made to the distance between the center of the platen and the center of the carrier head, when processing 450 mm wafers, at any given time, approximately 13.7% of the wafer hangs off the edge of the pad and hence does not contact the pad during polishing (see the darkened region in Fig. 2).

All wafers are polished for 1 minute on a Cabot Microelectronics Corporation D100 pad (concentrically grooved) at 3 pressures and 3 sliding velocities (Table I). Each run is repeated once. Since the distance between the center of the platen and the center of the carrier head is the same regardless of the size of wafers being polished, the rotational velocity of the head and the platen need not be adjusted for a given linear sliding velocity (Table I). This is important to note since in a real 450 mm polisher, the distance between the center of the platen and the center of the carrier head would be larger and hence a lower rotational velocity would be required to match the linear velocity to that of a 300 mm process. For instance, a real 450 mm polisher would have a platen that is 1,094 mm in diameter.<sup>6</sup> Therefore, to achieve a sliding velocity of 1 m/s, the larger platen would require an angular velocity of only 33 RPM compared to 42 RPM for the 300 mm system.

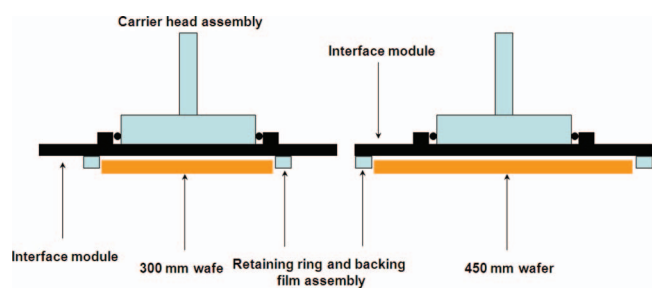
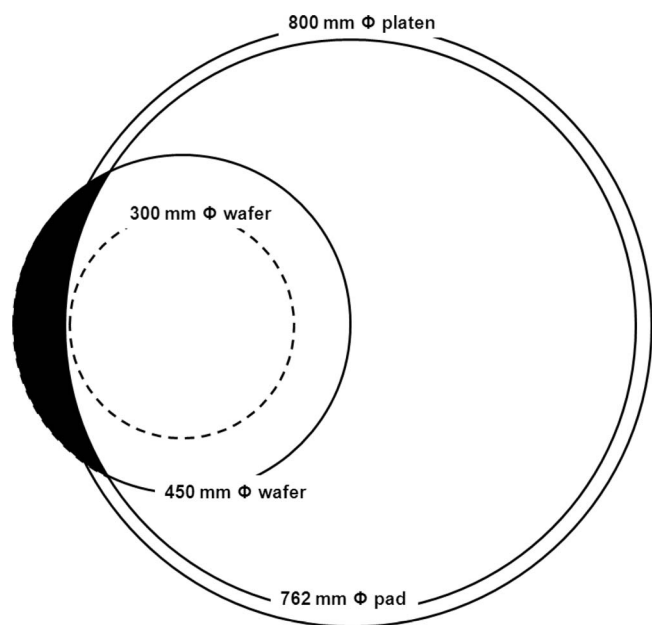
In addition to the runs summarized in Table I, two 85-second runs (one for each wafer size) are performed as per Table II. These runs allow accurate construction of the Stribeck curve within the range of parameters investigated.<sup>13</sup> Fujimi PL-4217 fumed silica slurry, with a point-of-use silica solids content of 10%, is used at a constant flow rate

\* Electrochemical Society Active Member.

<sup>z</sup> E-mail: jiao@email.arizona.edu

**Table I. Experimental conditions for each polishing run.**

| Run no. | Pressure (kPa) | Sliding Velocity (m/s) | Platen Angular Velocity (RPM) | Carrier Head Angular Velocity (RPM) |
|---------|----------------|------------------------|-------------------------------|-------------------------------------|
| 1       | P1 = 6.89      | V1 = 0.5               | $\Omega_p1 = 21$              | $\Omega_h1 = 18$                    |
| 2       | P1 = 6.89      | V2 = 1.0               | $\Omega_p2 = 42$              | $\Omega_h2 = 39$                    |
| 3       | P1 = 6.89      | V3 = 1.5               | $\Omega_p3 = 63$              | $\Omega_h3 = 61$                    |
| 4       | P2 = 13.79     | V1 = 0.5               | $\Omega_p1 = 21$              | $\Omega_h1 = 18$                    |
| 5       | P2 = 13.79     | V2 = 1.0               | $\Omega_p2 = 42$              | $\Omega_h2 = 39$                    |
| 6       | P2 = 13.79     | V3 = 1.5               | $\Omega_p3 = 63$              | $\Omega_h3 = 61$                    |
| 7       | P3 = 27.58     | V1 = 0.5               | $\Omega_p1 = 21$              | $\Omega_h1 = 18$                    |
| 8       | P3 = 27.58     | V2 = 1.0               | $\Omega_p2 = 42$              | $\Omega_h2 = 39$                    |
| 9       | P3 = 27.58     | V3 = 1.5               | $\Omega_p3 = 63$              | $\Omega_h3 = 61$                    |

**Figure 1.** Interface module for accommodating the 300 (left) and 450 mm (right) wafers.**Figure 2.** Position of the 300 and 450 mm wafers relative to the pad and the platen.**Table II. Experimental conditions for generating the Stribeck curve in a single polishing run.**

| Step no. | Pressure (kPa) | Sliding Velocity (m/s) | Time (Sec) |
|----------|----------------|------------------------|------------|
| 1        | P2 = 13.79     | V3 = 1.5               | T = 20     |
| 2        | P1 = 6.89      | V3 = 1.5               | T = 15     |
| 3        | P3 = 27.58     | V3 = 1.5               | T = 15     |
| 4        | P3 = 27.58     | V1 = 0.5               | T = 15     |
| 5        | P1 = 6.89      | V1 = 0.5               | T = 20     |

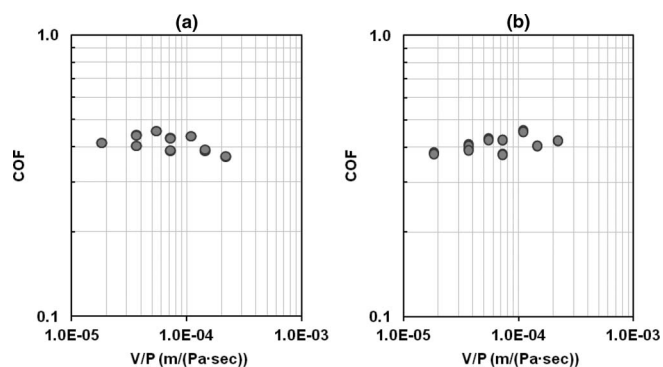
of 300 mL/min. The slurry is injected on the surface of the pad slightly off-center in order to clear the interface module. Prior to polishing, pad conditioning is performed (ex situ) using ultra-pure water (UPW) for 1 minute at 44.5 N down force with a rotation rate of 95 RPM and a sweep frequency of 10 times per minute. Prior to wafer polishing, the pad is broken in for 30 minutes using UPW followed by seasoning through polishing 5 dummy 300 or 450 mm wafers with slurry with ex-situ conditioning in between each run.

For each run, shear force (1,000 Hz acquisition frequency), down force (1,000 Hz acquisition frequency) and pad surface temperature (at the trailing edge of the interface module with 1 Hz acquisition frequency) are measured in real-time and reported as average coefficient of friction<sup>14</sup> as well as initial and final polish temperatures and the log-mean-temperature<sup>15</sup> for each run. The accuracy and precision of the FLIR infrared camera is  $\pm 0.5^\circ\text{C}$ .

## Results and Discussion

**Frictional studies.**— Fig. 3 shows Stribeck curves<sup>14</sup> (i.e. coefficient of friction, COF, vs. pseudo Sommerfeld number represented as the ratio of sliding velocity to the polishing pressure) for 300 and 450 mm systems. A total of 18 runs are performed for each wafer size. Results indicate that both systems are similar in terms of their frictional behavior. Also both processes are shown to operate in ‘boundary lubrication’ regime across the range of velocities and pressures investigated.

As the APD-800 is capable of measuring down force in real-time, the actual pressure, as opposed to the ‘dialed in’ pressure is also measured and reported at a rate of 1,000 Hz over a 85-second continuous run during which pressures and velocities are changed according to the recipe in Table II. Results (Fig. 4) again indicate that both systems behave similarly in terms of their tribological attributes and confirm that a single 85-second run during which pressure and velocity are

**Figure 3.** Stribeck curves based on 18 individual runs for the 300 mm system (a) and the 450 mm system (b).

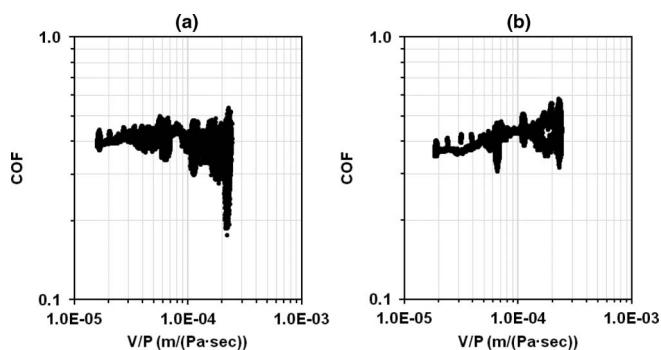


**Figure 4.** Stribeck curves based on one 85-second run for the 300 mm system (a) and the 450 mm system (b).

continuously varied and reported as 75,000 COF data points can be a viable and cost effective replacement for having to perform 18 separate polishing runs.<sup>13</sup> Additionally, Fig. 4 provides information about the range of COF values encountered during polishing as a result of stick-slip phenomena inherent to CMP. As shown in Fig. 4, depending on the particular choice of parameter values, the process experiences wide swings in COF thus alerting the user to stay away from these conditions to reduce process lateral vibration which has been known to cause low  $k$  dielectric films to delaminate during processing.<sup>16</sup>

**Thermal studies.**— Pad surface temperatures are shown in Fig. 5. The left y-axis represents the average trailing edge pad surface temperature near the beginning of the polishing step (i.e. at  $t = 5$  second) represented by the bottom of the bar, as well as near the end of the polish step (i.e.  $t = 55$  second) represented by the top of the bar. The log-mean-temperature (LMT)<sup>15</sup> of the process is represented by the white circle with the right y-axis and is calculated via Eq. 1:

$$LMT = \frac{(T_{55} - T_{ref}) - (T_5 - T_{ref})}{\ln\left(\frac{T_{55} - T_{ref}}{T_5 - T_{ref}}\right)} \quad [1]$$

where  $T_{ref}$  is the reference temperature (here taken as  $0^\circ\text{C}$ ). The x-axis represents  $P \times V$  values (corresponding to pressures and velocities reported in Table I) in ascending order. It is important to note that, in some cases, due to the particular test conditions selected, the same  $P \times V$  value is achieved with different conditions (i.e.  $P1 \times V2 = P2 \times V1$  and  $P3 \times V1 = P2 \times V2$ ). For clarity, these conditions are shown in darker color bars.

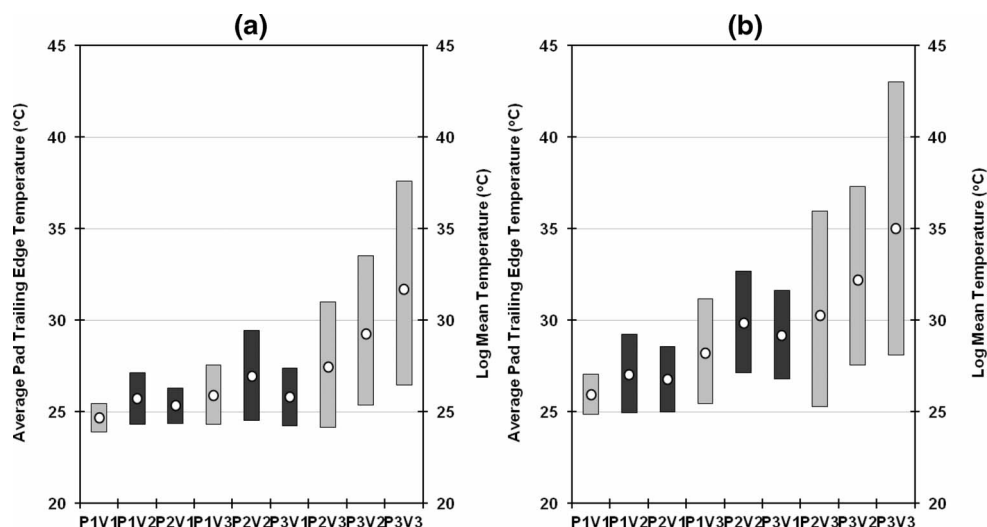


**Figure 5.** Average pad trailing edge temperatures (bars) and LMT (circles) as a function of  $P \times V$  for the 300 mm system (a) and the 450 mm system (b) ( $P1 = 6.9$  kPa,  $P2 = 13.8$  kPa,  $P3 = 27.6$  kPa,  $V1 = 0.5$  m/s,  $V2 = 1.0$  m/s,  $V3 = 1.5$  m/s)

For a given wafer size, results indicate higher values of LMT at higher values of  $P \times V$ . This is expected as higher  $P \times V$  values mean higher power inputs to the system which generate more heat due to friction. Results also show that, due to ‘boundary lubrication’ in all cases, for a given value of  $P \times V$ , neither pressure nor velocity dominate. That is, LMT associated with  $P2 \times V1$  is similar to that of  $P1 \times V2$ . The same holds for  $P3 \times V1$  vs.  $P2 \times V2$  conditions. Lastly, one can see the transient nature of temperature during a given run whereby average pad surface temperature can rise by as much as  $15^\circ\text{C}$  in just one minute. As for the effect of wafer size, Fig. 5 shows that, for a given  $P \times V$ , the 450 mm process runs warmer than the 300 mm process. Since for 450 mm polishing, a much larger wafer surface area contacts the pad ( $137,173$  mm<sup>2</sup> for the 450 mm system versus  $70,650$  mm<sup>2</sup> for the 300 mm system which corresponds to a 94 percent increase in contact area), more frictional heat is generated which causes the pad surface temperature to increase. This increase in temperature is minimal at low pressures and velocities (i.e.  $1$ – $2^\circ\text{C}$ ) and becomes significant at higher values of  $P \times V$  (i.e.  $4$ – $5^\circ\text{C}$ ).

LMT values vs.  $P \times V$  are shown in Fig. 6. Results indicate a straight line relationship exists between the two factors with the 450 mm system having a steeper slope ( $0.000260$  vs.  $0.000184^\circ\text{C per Pa} \cdot \text{m/s}$ ). As indicated earlier, comparing process temperatures between the two systems running at the same angular platen velocity,  $\Omega_p$ , is not appropriate since in a real 450 mm process, the platen would be rotating at a lower angular velocity than in a 300 mm process.<sup>6</sup> Fig. 6 also shows a straight line (without any data points) corresponding to the adjusted 450 mm temperature ( $LMT_{450\text{-adj}}$ ) with a slope that is lower than  $LMT_{450}$  by a factor of 1.27 which represents the ratio of the angular platen velocity of a 450 mm system<sup>6</sup> (i.e. 33 RPM) to that used in this study (i.e. 42 RPM). Since a linear relation exists between LMT and  $P \times V$  such a scaling is justified, therefore allowing one to compare the temperature of a 450 mm system to that of a 300 mm system. Based on the adjusted line, one can see that a 450 mm system will most likely operate at a higher wafer body temperature (by  $1$ – $3^\circ\text{C}$ ) than the 300 mm, especially at higher values of  $P \times V$ .

**Copper removal rate simulation studies.**— A 2-step modified Langmuir-Hinshelwood model<sup>7,9-11</sup> is used to simulate copper removal rate, wafer surface reaction temperature, and chemical and mechanical rate constants. In this model, it is assumed that  $n$  moles of reactant  $R$  in the slurry react with the copper surface film ( $S$ ) at rate  $k_1$  to form a surface layer  $L$ ,



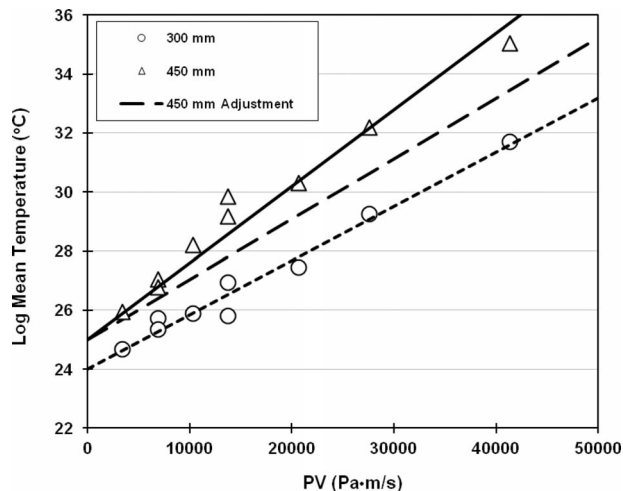


**Figure 6.** LMT and best straight line fits for 300 mm (circle) and 450 mm (triangle) wafers. The middle dashed line (no symbol) is the adjusted LMT for a 450 mm process.

This surface layer is then removed by mechanical abrasion with rate  $k_2$

$$\underline{L} \xrightarrow{k_2} L \quad [3]$$

The abraded material  $L$  is assumed to be carried away by the slurry and not re-deposited on the wafer surface. Assuming the rate of the surface layer formation is equal to the rate of its depletion, the local removal rate in this sequential mechanism is

$$RR = \frac{M_w}{\rho} \frac{k_1 C_R^n}{1 + \frac{k_1 C_R^n}{k_2}} \quad [4]$$

where  $C_R$  is the local molar concentration of the reactant  $R$ . To simplify the model, it is assumed that there is no reactant depletion so that  $C_R$  remains constant in Equation 4. This allows  $C_R$  to be absorbed into  $k_1$  and its value is set to be unity as

$$RR = \frac{M_w}{\rho} \frac{k_1 k_2}{k_1 + k_2} \quad [5]$$

The chemical reaction rate constant  $k_1$  in Equation 5 is expressed as

$$k_1 = A \exp(-E/kT_w) \quad [6]$$

where  $A$  is an exponential factor,  $E$  is the slurry activation energy,  $k$  is a constant ( $8.62 \times 10^{-5}$  eV/K), and  $T_w$  is the wafer surface reaction temperature.

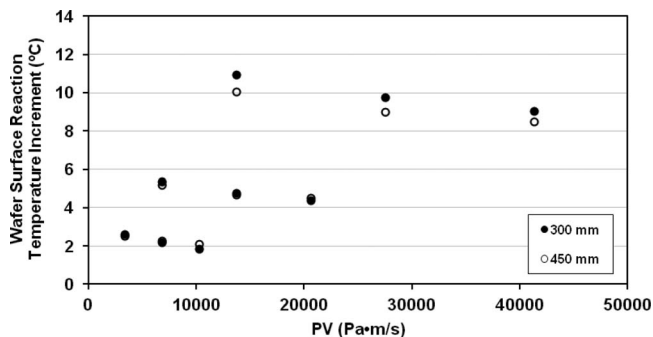


**Figure 7.** Simulated wafer surface reaction temperature increment as a function of  $P \times V$  for 300 mm and 450 mm wafers.

**Table III.** Values of  $E$ ,  $A$ ,  $C_p$ ,  $\beta$ , and  $e$  used in removal rate simulation.

|   |                       |
|---|-----------------------|
| $E$ (eV)  | 1.2                   |
| $A$ (mole $\cdot$ m $^{-2}$ $\cdot$ s $^{-1}$ ) | $5.39 \times 10^{16}$ |
| $C_p$ (mole/J)                                  | $2.26 \times 10^{-7}$ |
| $\beta$ (K/Pa $\cdot$ (m/s) $^{e-0.5}$ )        | $0.80 \times 10^{-3}$ |
| $e$   | 0.76                  |

The mechanical removal rate constant  $k_2$  in Equation 5 is expressed as

$$k_2 = c_p \mu_k p V \quad [7]$$

where  $C_p$  is a proportionality constant and  $\mu_k$  is the COF.

Assuming the chemical reaction is determined by transient flash heating, the wafer surface reaction temperature ( $T_w$ ) in Equation 6 is expressed as

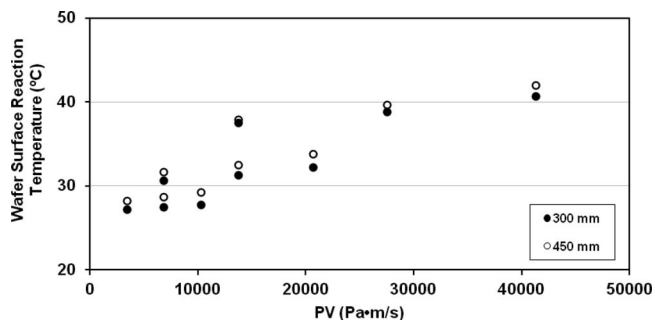
$$T_w = T_p + \frac{\beta}{V^{1/2+e}} \mu_k p V \quad [8]$$

where  $T_p$  is the pad surface temperature (as reported in Fig. 5),  $\beta$  is a grouping of parameters including the contact area fraction and associated pad properties, and  $e$  is an exponential factor.

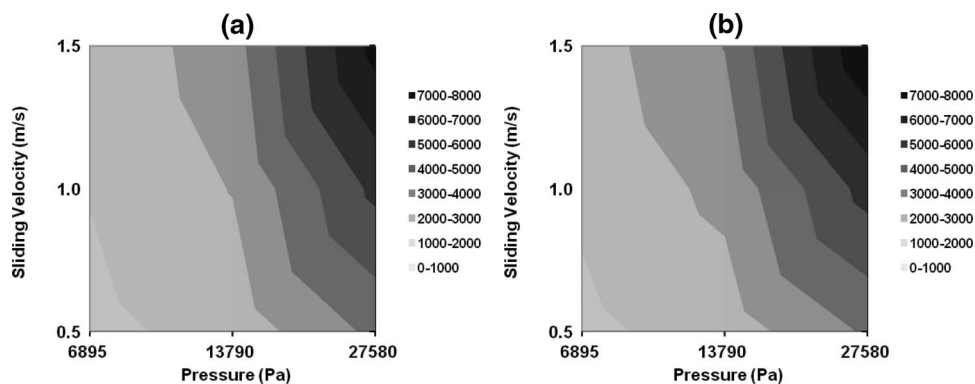
The values for parameters  $A$ ,  $C_p$ ,  $\beta$ , and  $e$ , as well as the slurry activation energy, are listed in Table III. These are based on successful simulations that we have recently performed (with relative root mean square error values of less than 2-5%) on our 300 mm polisher using the same pad and diamond disk as in this study.<sup>11</sup>

Fig. 7 shows the simulated wafer surface reaction temperature increment as a function of  $P \times V$  for wafers of both sizes. Fig. 8 shows the wafer surface reaction temperature which is simply the sum of the wafer surface reaction temperature increment and the LMT value for 300 mm wafers, and the sum of the surface reaction temperature increment and the adjusted LMT for the 450 mm wafers. Results basically show that both systems have similar surface reaction temperatures across the board and that the 450 mm system runs slightly warmer (by 1–2°C).

The above mentioned temperature difference between the 2 sizes manifests itself as higher copper removal rates for the 450 mm system as shown in the Lim-Ashby plots of Fig. 9. In both cases, at moderate values of  $P \times V$ , pressure dominates removal rate as evidenced by the near vertical contours at the center of the plots. At low and high values of  $P \times V$ , pressure and sliding velocity contribute equally to removal rate. At most polishing conditions, the copper removal rates for the 450 mm process are slightly higher (2–13%) than that of the 300 mm process.



**Figure 8.** Wafer surface reaction temperature for 300 mm and 450 mm wafers.



**Figure 9.** Lim-Ashby contour plots of simulated copper removal rate (in Angstroms per minute) vs. sliding velocity and process pressure for 300 mm (a) and 450 mm (b) wafers.

### Conclusions

In this study, an existing 300 mm CMP tool is modified to polish 450 mm wafers to experimentally investigate whether any differences exist in the tribological and thermal characteristics of the two processes, and from that, to infer whether one can expect any removal rate differences between the two systems. The tribological study indicates that, within the ranges of parameter investigated, the two systems behave similarly in terms of their coefficients of friction and lubrication regimes. Additionally, it is shown that the 450 mm process, once adjusted for its platen velocity, runs only slightly warmer (by 1-3°C) than its 300 mm counterpart. Experimental data, coupled with copper removal rate simulations show that the wafer surface reaction temperature for the 450 mm process is slightly higher (by 1-2°C) than the 300 mm process. Consequently, simulated copper removal rates for the 450 mm process are slightly higher than those of the 300 mm process at most polishing conditions. The above results indicate that when the current 300 mm CMP process is scaled up to 450 mm, the tribological, thermal, and kinetic attributes of the process remain similar and do not undergo significant changes. As a result, it is expected that a smooth transition can be achieved by IC makers in this CMP scaling up process.

### Acknowledgments

The authors thank the SRC/SEMATECH Engineering Research Center for Environmental Benign Semiconductor Manufacturing for providing the financial support for this work.

### References

- <http://blog.timesunion.com/capitol/archives/82186/cuomo-announces-intel-ibm-will-partner-at-nanocollege/>.
- <http://semiconwest.org/node/6371>.
- [http://www.semi.org/en/IndustrySegments/WaferProcessing/ssLINK/CTR\\_041227](http://www.semi.org/en/IndustrySegments/WaferProcessing/ssLINK/CTR_041227).
- M. Watanabe and S. Kramer, *The Electrochemical Society Interface*, pp. 28-31, winter (2006).
- J.S. Pettinato and D. Pillai, *IEEE Trans. Semicond. Manuf.*, **18**(4), 501, (2005).
- L. Borucki, A. Philipossian, and M. Goldstein, *Solid State Technol.*, **52**(12), 10 (2009).
- J. Sorooshian, L. Borucki, R. Timon, D. Stein, D. Hetherington, and A. Philipossian, *J. Tribol.*, **127**, 639 (2005).
- T. Sun, L. Borucki, Y. Zhuang, Y. Sampurno, F. Sudargho, X. Wei, S. Anjur, and A. Philipossian, *Jpn. J. Appl. Phys.*, **49**, 026501 (2010).
- D. Rosales-Yeomans, L. Borucki, T. Doi, L. Lujan, and A. Philipossian, *J. Electrochem. Soc.*, **153**(4), G272 (2006).
- Y. Zhuang, L. Borucki, E. Dien, M. Ennahali, G. Michel, B. Laborie, D. Rosales-Yeomans, H. Lee, and A. Philipossian, *Trans. Electr. Electron. Mater.*, **8**(2), 53 (2007).
- Y. Jiao, Y. Sampurno, Y. Zhuang, X. Wei, A. Meled, and A. Philipossian, *Jpn. J. Appl. Phys.*, **50**, 05EC02 (2011).
- <http://aracinc.com/products/apd-800>.
- Y. Sampurno, S. Theng, F. Sudargho, Y. Zhuang, and A. Philipossian, "Method for Ultra-rapid Determination of the Lubrication Mechanism of CMP Processes", presented at *Material Research Society Spring Meeting*, San Francisco, CA (2010).
- A. Philipossian and S. Olsen, *Jpn. J. Appl. Phys.*, **42**, 6371 (2003).
- W.L. McCabe, J.C. Smith, and P. Harriott, *Unit Operations of Chemical Engineering*, p. 333, McGraw Hill Chemical Series, 7th ed. (2005).
- Y. Sampurno, T. Nemoto, Y. Zhuang, S. Theng, X. Gu, T. Ohmi, and A. Philipossian, "Optimizing Pad Groove Design and Polishing Kinematics for Reduced Shear Force, Low Force Fluctuation and High Removal Rate Attributes of Copper CMP", *International Conference on Planarization/CMP Technology*, Fukuoka, Japan (2009).